

Decision-making for Autonomous Vehicles on Highway: Deep Reinforcement Learning with Continuous Action Horizon

Xin Ye, Xiaolin Tang, Kang Yu

Abstract—Decision-making strategy for autonomous vehicles describes a sequence of driving maneuvers to achieve a certain navigational mission. This paper utilizes the deep reinforcement learning (DRL) method to address the continuous-horizon decision-making problem on the highway. First, the vehicle kinematics and driving scenario on the freeway are introduced. The running objective of the ego automated vehicle is to execute an efficient and smooth policy without collision. Then, the particular algorithm named proximal policy optimization (PPO)-enhanced DRL is illustrated. To overcome the challenges in tardy training efficiency and sample inefficiency, this applied algorithm could realize high learning efficiency and excellent control performance. Finally, the PPO-DRL-based decision-making strategy is estimated from multiple perspectives, including the optimality, learning efficiency, and adaptability. Its potential for online application is discussed by applying it to similar driving scenarios.

Index Terms—Autonomous vehicles, decision-making, proximal policy optimization, deep reinforcement learning, continuous action horizon

NOMENCLATURE

DRL	Deep Reinforcement Learning
PPO	Proximal Policy Optimization
AI	Artificial Intelligence
AD	Autonomous Driving
MDP	Markov Decision Process
NN	Neural Network
RL	Reinforcement Learning
DQL	Deep Q-learning
AEV	Autonomous Ego Vehicle

This work was supported by the Science and Technology Innovation Key R&D Program of Chongqing (No. CSTB2022TIAD-STX0005) (Corresponding authors: X. Tang)

X. Ye is with Vehicle Engineering Institute, Chongqing University of Technology, Chongqing 40054, China, and also with Key Laboratory of Advanced Manufacturing Technology for Automobile Parts of Ministry of Education, Chongqing University of Technology, Chongqing 400054, China. (email: yexin@cqut.edu.cn)

X. Tang is with College of Mechanical and Vehicle Engineering, Chongqing University, Chongqing, 400044, China. (email: tangxiaolin6@126.com)

K. Yu is with Vehicle Engineering Institute, Chongqing University of Technology, Chongqing 40054, China. (email: yukang07@outlook.com)

IDM	Intelligent Driver Model
MOBIL	Minimize Overall Braking Induced by Lane Changes
ACC	Adaptive Cruise Control
SGD	Stochastic Gradient Descent
CEM	Cross-Entropy Method

I. INTRODUCTION

MOTIVATED by advanced artificial intelligence (AI) technologies, autonomous vehicles are becoming promising transportation means to ameliorate traffic accidents and promote road efficiency [1]-[2]. Four pivotal modules are necessary for an automated vehicle, which are perception, decision-making, planning, and control [3]-[4]. To achieve full automation in complex driving scenarios, more efforts are required in these research fields.

Decision-making indicates a continuous sequence of driving maneuvers to realize certain navigational tasks [5]-[6]. The special instructions contained in a decision-making strategy are usually accelerator pedal and steering angle. Many attempts have been implemented to deduce an appropriate decision-making policy. For example, Hoel et al. [7] conducted a Monte Carlo tree search to derive tactical decision-making for autonomous driving (AD). The driving environment is partially observable Markov decision process (MDP), and the relevant results are compared with the neural network (NN) policy. The authors discussed the cooperative lane changing decisions to leverage limited road resources and reduce competition [8]. Furthermore, Ref. [9] described the highway-exit decisions for autonomous vehicles. The authors claimed the presented decision-making controller achieves a higher probability of successful highway exiting with 6000 times of stochastic simulations.

Reinforcement learning (RL), especially deep reinforcement learning (DRL) methods, exhibit powerful potentials to dispose of the decision-making problems in AD [10]. For example, the authors in [11] applied deep Q-learning (DQL) to handle the lane changing decision-making problem in an uncertain highway environment. Same for the lane changing problem, Zhang et al. [12] developed a model-based exploration policy according to surprise intrinsic reward. Furthermore, Ref. [13] surveyed the existing applications of RL or DRL for automated vehicles, including training agents, evaluation techniques, and robust estimation. However, several drawbacks restricted the real-world applications of DRL-based decision-making strategies, such as sample efficiency, slow learning rates, and operation safety.

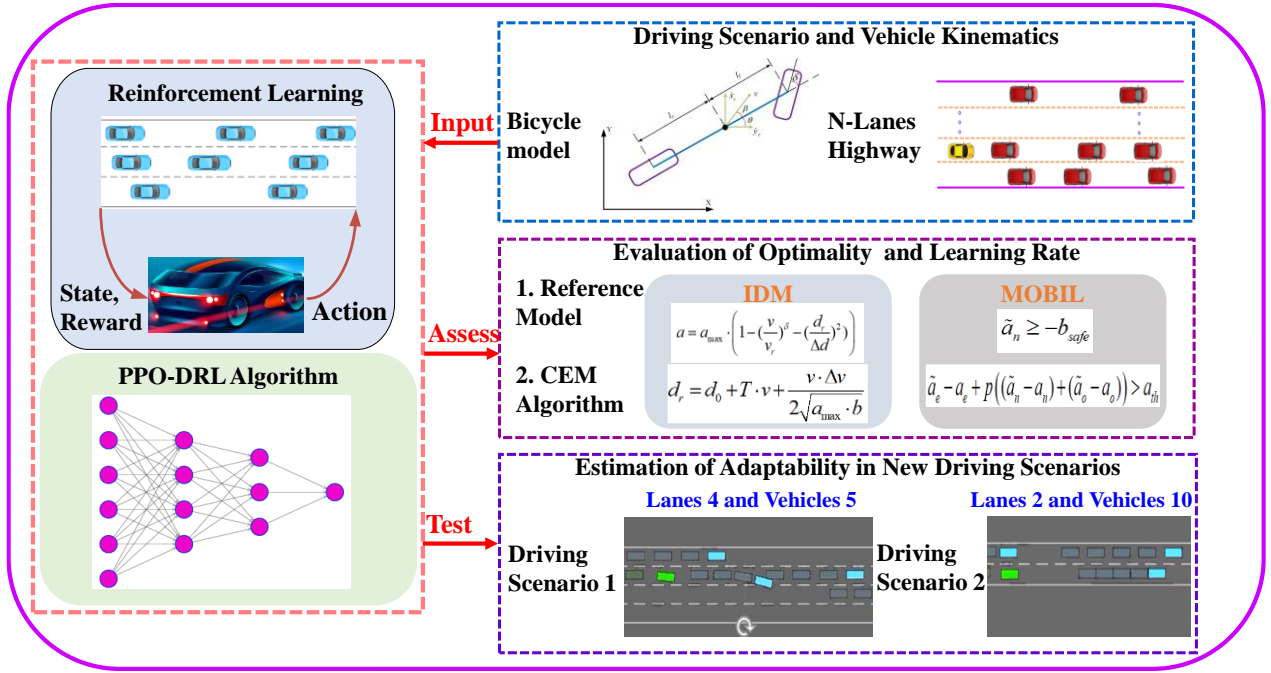


Fig. 1. An efficient and safe decision-making control framework based on PPO-DRL for autonomous vehicles.

To derive an efficient and safe decision-making policy for AD, this work presents a proximal policy optimization (PPO)-enhanced DRL approach on the highway with a continuous action horizon, as depicted in Fig. 1. We first establish the vehicle kinematics and driving scenarios, in which the studied autonomous ego vehicle aims to run efficiently and safely. Having the ability to obtain control actions directly from the policy gradient method, PPO-enabled DRL can enforce a trust region with clipped objectives. The detailed realization of this DRL algorithm is explained afterward. Finally, a series of test experiments are designed to evaluate the optimality, learning efficiency, and adaptability of the related decision-making policy on the highway.

Three perspectives of contributions and innovations have appeared in this work: 1) an advanced efficient and safe decision-making policy is built for AD on the highway; 2) the PPO-enhanced DRL is utilized to resolve the transferred control optimization problem for autonomous vehicles; 3) an adaptive estimation framework is founded to test the adaptability of the proposed approach. This work is one attempt to address the efficiency and safety of decision-making policy with the emerging advanced DRL method.

To better explain the contributions of this article, the rest of this work is arranged as follows. Section II describes the vehicle kinematics and driving scenarios on the highway. The research PPO-enhanced DRL is explained in Section III. Section IV analyzes the relevant simulation results of the presented decision-making strategy. Finally, the concluding remarks are provided in Section V.

II. VEHICLE KINEMATICS AND DRIVING SCENARIOS

In this section, the research highway driving scenario is established. This environment includes the autonomous ego vehicle (AEV) and its surrounding vehicles. The vehicle kinematics of these vehicles are also described. Hence, the longi-

tudinal and lateral speeds can be calculated. Furthermore, the reference models for driving maneuvers at the longitudinal and lateral direction are introduced.

A. Vehicle Kinematics

In this work, the vehicle kinematics is described by the common bicycle model [14]-[15], which are the nonlinear continuous horizon equations. The representation of the inertial frame is depicted in Fig. 2. The differentials of position and inertial heading are computed as follows:

$$\dot{x} = v \cos(\psi + \beta) \quad (1)$$

$$\dot{y} = v \sin(\psi + \beta) \quad (2)$$

$$\dot{\psi} = \frac{v}{l_r} \sin \beta \quad (3)$$

where (x, y) is the position coordinate of the vehicle in the inertial frame. v is the vehicle velocity and l_r is the distance between the center of the mass and rear axles. ψ is the inertial heading, and β is a slip angle at the center of gravity. This angle and the vehicle speed can be further displayed as:

$$\dot{v} = a \quad (4)$$

$$\beta = \arctan \left(\frac{l_r}{l_f + l_r} \tan(\delta_f) \right) \quad (5)$$

where l_f is the distance of the center of mass with respect to the front. δ_f is front steering angles. The two degrees-of-freedom model is easy enough to delegate the main parameters of the vehicle, speed and acceleration. The control inputs of this model are the acceleration and steering angle which are continuous time horizon in this article.

The default parameters of the AEV and surrounding vehicles are the same. The length and width are 5.0 m and 2.0 m, respectively. The initial speed is randomly chosen from [23, 25] m/s, and the maximum value of the speed is 30 m/s. The orig-

inal position is randomly given on the highway, which indicates the uncertainty of the driving environment.

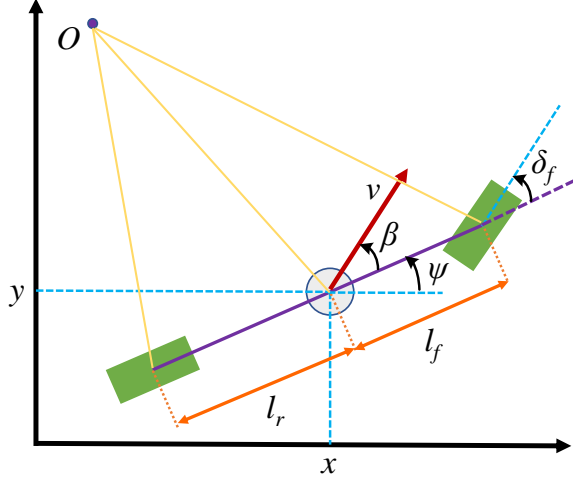


Fig. 2. Bicycle model for vehicle kinematics on highway.

B. Driving Scenarios

To mimic the practical driving environment on highway, a driving scenario with N lane in the same direction is constructed, as depicted in Fig. 3. The Decision-making strategy for AEV in this work indicates determining the control actions of vehicle speed and steering angle at each time step. The core objective of the AEV is to drive as fast as possible without crashing the surrounding vehicles.

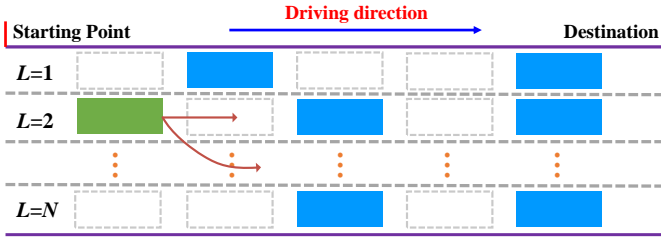


Fig. 3. Driving scenario on highway with N lanes for decision-making policy.

Overtaking behavior represents that the studied vehicle surpasses the nearby vehicles via lane-changing and accelerating maneuvers. In general, three indicators are often used to evaluate the performance of decision-making policy, which are safety, efficiency, and comfort. Safety means the AEV should avoid a collision. Efficiency implies that an autonomous vehicle prefers to increase speed. Comfort indicates the AEV should regulate the frequency of lane-changing and the value of vehicle deceleration [16].

In this work, the key concerns of the AEV are safety and efficiency. This vehicle also prefers to locate on the high-speed lane. As shown in Fig. 3, the green vehicle is AEV, and the blue vehicles are the surrounding vehicles. In each lane, the number of the surrounding vehicles is K . One episode in this article indicates the AEV overtakes all the surrounding vehicles or reaches the destination.

Without loss of generality, the number of lanes on the highway is set as $N=3$. The number of surrounding vehicles in

each lane is set to $K=5$. The predefined lane of the AEV is the right lane. The simulation frequency is 20 Hz, and the sampling time is 1 second (means the AEV chooses action every one second). The duration of one episode is 50 seconds. The driving maneuvers of the surrounding vehicles are managed by two common models, which will be introduced in the next subsection.

C. Behavioral Controller

In this part, the intelligent driver model (IDM) and minimize overall braking induced by lane changes (MOBIL) are formulated to manipulate the driving behaviors of surrounding vehicles. Moreover, the combination of these two models is taken as a reference model for the AEV to compare with the proposed DRL method.

IDM is usually utilized for adaptive cruise control (ACC) of automated vehicles as a continuous-time horizon car-following model [17]-[18]. The longitudinal acceleration in IDM is described as follows:

$$a = a_{\max} \cdot \left(1 - \left(\frac{v}{v_r} \right)^{\delta} - \left(\frac{d_r}{\Delta d} \right)^2 \right) \quad (6)$$

where a_{\max} is the maximum acceleration. v_r and d_r are the request vehicle velocity and separation distance. δ is the constant acceleration parameter, and Δd is the interval between the studied vehicle and the leading vehicle. In IDM, the requested speed is decided by the maximum acceleration and request distance, and this distance is further calculated as:

$$d_r = d_0 + T \cdot v + \frac{v \cdot \Delta v}{2\sqrt{a_{\max} \cdot b}} \quad (7)$$

where d_0 is the minimum relative distance between two vehicles on the same lane, and T is the desired time interval for the safety objective. Δv is the relative speed gap between the research vehicle and its front one, and b is the value of deceleration according to the comfortable purpose. The parameters of the IDM in this work is depicted in Table I.

TABLE I
DEFAULT PARAMETERS OF IDM

Symbol	Value	Unit
Maximum acceleration a_{\max}	6	m/s ²
Acceleration argument δ	4	/
Desired time gap T	1.5	s
Comfortable deceleration rate b	-5	m/s ²
Minimum relative distance d_0	10	m

After determining the longitudinal acceleration of the surrounding vehicle, MOBIL is applied to regulate the lateral lane-changing decisions [19]. Two conditions constitute the constraints in MOBIL, which are safety criterion and incentive condition. The safety criterion states that when the lane changing occurs, the new following vehicle should not decelerate too much to avoid the collision. The acceleration expression is shown as follows:

$$\tilde{a}_n \geq -b_{safe} \quad (8)$$

where \tilde{a}_n is the acceleration of the new follower after lane changing. b_{safe} is the maximum deceleration imposed on the new follower. (8) is leveraged to ensure collision-free conditions.

Assuming the a_n and \tilde{a}_n are the accelerations of the new follower before and after lane-changing, a_o and \tilde{a}_o are the accelerations of the old follower before and after lane-changing. The incentive condition is represented by the restraint on the acceleration as follows:

$$\tilde{a}_e - a_e + p((\tilde{a}_n - a_n) + (\tilde{a}_o - a_o)) > a_{th} \quad (9)$$

where a_e and \tilde{a}_e are the accelerations of the AEV before and after lane-changing. p is the politeness coefficient to determine the effect degree of the followers in the lane-changing process. a_{th} is the lane-changing decision threshold. This condition implies that the desired lane should be safer than the old one. It should be noticed the accelerations in MOBIL are decided by IDM at each time instant. Furthermore, the AEV could overtake the surrounding vehicles from the right and left lanes. The parameters of MOBIL are depicted in Table II.

TABLE II
MOBIL CONFIGURATION

Keyword	Value	Unit
Safe deceleration limitation b_{safe}	2	m/s ²
Politeness factor p	0.001	/
Lane-changing decision threshold a_{th}	0.2	m/s ²

III. PROXIMAL POLICY OPTIMIZATION-ENABLED DEEP REINFORCEMENT LEARNING

This section interprets the realization procedure of the studied PPO-enhanced DRL method. First, the preliminaries of the reinforcement learning (RL) methods and the necessity of continuous-time horizon are introduced. Then, the usual form of the policy gradient technique is explained. Finally, the PPO-enabled DRL is illuminated to derive the decision-making strategy for the control problem constructed in Section II.

A. Necessity of Continuous Horizon

RL is an emerging methodology to address the sequential decision-making problem via trial and error process [20]-[22]. This course is reflected by the interaction between an intelligent agent and its environment. The agent adopted a control action to the environment and received the evaluation of this choice from the environment [23]-[24]. In general, RL methods are classified into policy-based ones (i.e., policy gradients algorithm) and value-based ones (i.e., Q-learning and Sarsa algorithms).

In the decision-making problem on the highway, the intelligent agent is the decision-making controller of the AEV, and the environments are interpreted as the surrounding vehicles. The interaction between them is usually mimicked by the Markov decision processes (MDPs) with Markov property [25]. The keyword of the MDP is a tuple $(\mathcal{S}, \mathcal{A}, \mathbf{P}, \mathbf{R}, \gamma)$, wherein \mathcal{S} and \mathcal{A} are the sets of state variable and control actions. \mathbf{P} is the transition model of the state variable, and \mathbf{R} is the reward model related to the state-action pair (s, a) . γ is called a discount factor to achieve a trade-off between current and future rewards.

The objective of RL techniques is selecting a sequence of control actions from \mathcal{A} to maximize the cumulative rewards. This accumulated rewards R_t is the sum of the current reward and the discounted future rewards as:

$$R_t = \sum_{t'=0}^{\infty} \gamma^{t'} \cdot r_{t'} \quad (10)$$

where t is the time step, and r_t is the relevant instantaneous reward. Two value functions are formulated to represent the worth of the control action selection. They are named as state-value function V and state-action function Q :

$$V^\pi(s_t) \doteq E_\pi[R_t | s_t, \pi] \quad (11)$$

$$Q^\pi(s_t, a_t) \doteq E_\pi[R_t | s_t, a_t, \pi] \quad (12)$$

where π is a special control policy. As can be seen, different control policies lead to diverse worth of value function, the best performance is welcome. The optimal control policy is described as follows:

$$\pi(s_t) = \arg \max_{a_t} Q(s_t, a_t) \quad (13)$$

The essence of the RL algorithms is updating the value functions according to the interactions between the agent and environments [26]. The value function then helps the agent find the optimal control strategy. For DRL, the value function is approximated by the neural network. From (12), it is obvious that the state-action function is a matrix, and its rows and columns are the numbers of state variables and control actions. For the problem with enormous spaces of state variables and control actions, it is inefficient to update the value function and search the control policy.

To overcome this drawback, this work simulates the control actions as a vehicle throttle and steering angle. The throttle affects the acceleration, and the steering angle influences the lane-changing behavior directly. Moreover, these two actions have continuous-time horizons, which are $[-5, 5]$ m/s² and $[-\Pi/4, \Pi/4]$ rad (Π is the circumference as 3.1415). By doing this, the AEV could decide the control action pair at each time step and thus determine the vehicle kinematics in Section II.A.

B. Policy Gradient

For policy-based RL methods, an estimator of the policy gradient is computed along with a stochastic policy and depicted as follows:

$$\hat{g} = \hat{E}_t \left[\nabla_\theta \log \pi_\theta(a_t | s_t) \hat{A}_t \right] \quad (14)$$

where \hat{E}_t indicates the expectation over a finite batch of samples, π_θ is a random control policy, and \hat{A}_t implies the advantage function. To compute the estimator of the policy gradient, the loss function of updating a RL policy is described as:

$$L^{PG}(\theta) = \hat{E}_t \left[\log \pi_\theta(a_t | s_t) \hat{A}_t \right] \quad (15)$$

In the common policy gradient method, this loss function L^{PG} is applied to perform multiple steps of optimization with the same control policy. However, some challenges may happen in the updating process of huge policy, such as sample inefficiency, policy diversity, and hesitation in exploration and exploitation. To address these challenges, a PPO algorithm is

proposed in [27] to combine the merits of typical value-based and policy-based RL methods.

C. PPO DRL

In the traditional policy gradient approach, the policy is able to be altered tempestuously in each updating. To avoid this operation, a policy surrogate objective is modified as the following form:

$$L^{CLIP}(\theta) = \hat{E}_t \left[\min(r_t(\theta)\hat{A}_t, \text{clip}(r_t(\theta), 1-\tau, 1+\tau))\hat{A}_t \right] \quad (16)$$

where

$$r_t(\theta) = \frac{\pi_\theta(a_t | s_t)}{\pi_{\theta_{old}}(a_t | s_t)} \quad (17)$$

where $r_t(\theta)$ denotes the probability ratio. Two terms are compared in (16), wherein the first term is the surrogate objective [28], and the second term revises this surrogate objective by clipping the probability ratio. τ is a hyperparameter with a value of 0.2. In the second term, the probability ratio $r_t(\theta)$ is clipped from $1-\tau$ to $1+\tau$, and composes the clipped objective via multiplying the advantage function. Adding this clipped version could effectively avoid taking a large policy updating from the old policy.

To share parameters between the policy and value functions through a neural network, the loss function is rewritten as the combination of policy surrogate and a value function error term [27]. This new loss function is formed as follows:

$$L^{CLIP+VF+S}(\theta) = \hat{E}_t \left[L_t^{CLIP}(\theta) - c_1 L_t^{VF}(\theta) - c_2 S[\pi_\theta](s_t) \right] \quad (18)$$

where $L_t^{VF}(\theta)$ is the squared-error loss of the state-value function $(V_\theta(s_t) - V_t^{tar})^2$, S indicates an entropy loss. c_1 and c_2 are the coefficients.

TABLE III
IMPLEMENTATION CODE OF PPO ALGORITHM

PPO Algorithm, Actor-Critic Style	
1.	For iteration = 1, 2, ..., do
2.	For actor = 1, 2, ..., M do
3.	Run policy $\pi_{\theta_{old}}$ in environment for T timesteps
4.	Calculate advantage function based on (19)-(20), $\hat{A}_1, \dots, \hat{A}_T$
5.	end for
6.	Optimize loss function in (18) with respect to θ for Z epochs
7.	Update θ_{old} with θ
8.	end for

To estimate the advantage function, a T timesteps (T is much less than the episode length) data is sampled. This collected data is utilized to update the loss function, in which the advantage function has a truncated version as:

$$\hat{A}_t = \delta_t + (\gamma\lambda)\delta_{t+1} + \dots + (\gamma\lambda)^{T-t} \delta_{T-1} \quad (19)$$

where

$$\delta_t = r_t + \gamma V(s_{t+1}) - V(s_t) \quad (20)$$

In each iteration, M actors are built to collect the T timesteps data. λ is the discounting factor for the advantage function. Then, the surrogate loss is constructed by these collected data and optimized with mini-batch stochastic gradient descent

(SGD) for Z epochs. The realization pseudo-code of the PPO algorithm is described in Table III.

As explained in Section III.A, the control actions are the vehicle throttle and steering angle. They have a continuous time horizon. The state variables are the speed of the AEV, the position of the AEV, and the relative speed and position between the AEV and its surrounding vehicles:

$$\Delta s = |s_{aev} - s_{sur}| \quad (21)$$

$$\Delta v = |v_{aev} - v_{sur}| \quad (22)$$

where s and v are the position and speed information obtained from (1)-(5) in Section II.A. The superscript *aev* and *sur* indicate the AEV and surrounding vehicles, respectively. The expressions (21) and (22) can also be treated as the transition model \mathbf{P} in the RL framework.

Finally, the reward function \mathbf{R} in this article includes three items, which reflect the efficiency, safety, and preferred lane objectives. Specifically, the AEV should drive as fast as possible, prefer to stay on the right lane, and avoid crashing other surrounding vehicles. The instantaneous reward at time step t is defined as follows:

$$r_t = -100 \cdot collision - 40 * (L-1)^2 - 10 * (v_{aev} - v_{aev}^{max})^2 \quad (23)$$

where $collision \in \{0, 1\}$ indicates the collision conditions for the AEV. $L \in \{1, 2, 3\}$ implies the lane number. For compared convenience, the value of the instantaneous reward is mapped to the range $[0, 1]$ at each step. It means the maximum value of the cumulative rewards for one episode equal to the duration time (set as 50 in this work) of the driving scenario.

The default parameters for the presented PPO-enhanced DRL method are defined as follows: The discount factor γ and learning rate α in the RL framework are 0.8 and 0.01. The training timesteps N is 51200, the mini-batch size Z is 64, the hyperparameter τ is 0.2, and the discounting coefficient for advantage function λ is 0.92. The decision-making policy on the highway for the AEV is derived and estimated in the OpenAI gym Python toolkit [29]. The control performance of this proposed decision-making strategy is discussed and analyzed in the next section.

IV. EXPERIMENTS AND DISCUSSION

This section evaluates the control performance of the proposed PPO-DRL-based decision-making strategy for the AEV. The estimation contains three aspects. First, the effectiveness of this decision-making policy is compared and certified with two other methods. The detailed simulation results imply its optimality. Second, the learning ability of the proposed PPO algorithm is proven by analyzing the loss function and accumulated rewards. Finally, the derived decision-making policy is assessed in two similar driving scenarios on the highway to state its adaptability.

A. Effectiveness of PPO DRL

Three methods for decision-making problems on the highway are compared in this subsection. They are PPO-DRL, reference model (IDM+MOBIL), and cross-entropy method (CEM). CEM is proven to be effective for continuous-time horizon problem in [30]. The reference model and CEM are regarded as the benchmark approaches to deduce the optimality

of the PPO-DRL algorithm. The setting parameters in PPO and CEM are the same.

The total reward acquired in each episode could mostly manifest the performance of control policy in DRL. The normalized average rewards in these three compared techniques are described in Fig. 4. The increasing trend of these curves indicates the AEV could learn to run better via interacting with the environment. It also can be discerned that the learning rate of PPO-DRL is better than the other two methods. Its rewards are always greater than those in CEM and IDM+MOBIL. Hence, the control policy obtained by PPO is superior to the other two strategies.

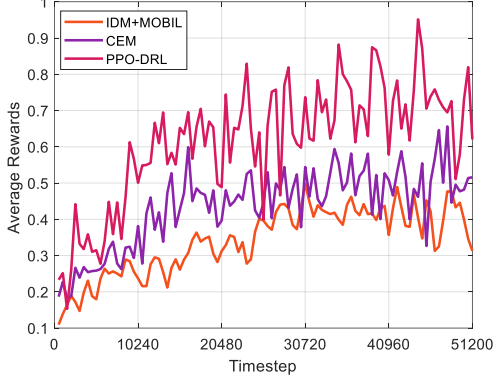


Fig. 4. Normalized average rewards in the reference model, CEM, and PPO-DRL for comparison purposes.

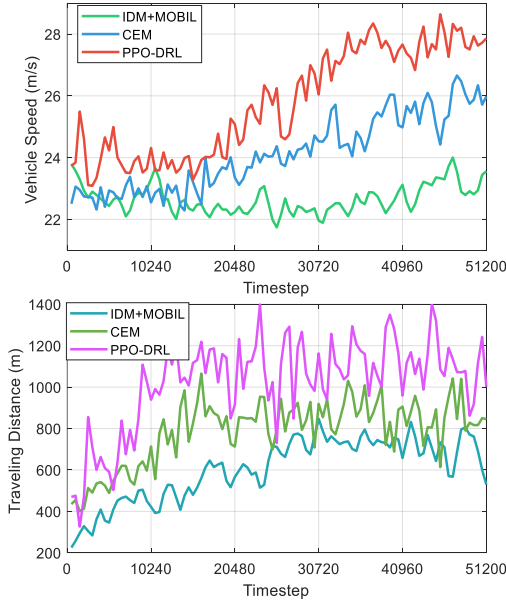


Fig. 5. Vehicle speed and traveling distance of the AEV in three methods.

Since the vehicle speed and distance are chosen as the state variables in this work, Fig. 5 depicts the varied trajectories of these variables. In (23), the reward function requests the AEV boosts its speed at appropriate places. Thus, the higher speed means larger rewards. The longer traveling distance of the AEV indicates the selected control actions enable this vehicle to run longer and avoid a collision. These simulation results imply that the AEV guided by PPO-DRL could achieve efficiency and safety goals effectively.

Finally, to compare the performance of these three methods

in collision-free conditions, Table IV describes the collision rate and success rate in the testing episodes (the number of testing episodes is 100). Collision rate indicates the probability of a crash happens, and the success rate means the AEV surpasses all the surrounding vehicles and reaches the destination. It is obvious that the PPO-DRL could avoid collision effectively than the other two methods. The value of success rate also implies that the PPO algorithm is capable of finishing the driving task in an efficient manner.

TABLE IV
COLLISION CONDITIONS IN THREE COMPARED APPROACHES

Algorithms	Collision rate (%)	Success rate (%)
PPO-DRL	0.59	99.03
CEM	4.32	91.55
IDM+MOBIL	7.10	87.21

B. Learning rate of PPO DRL

In this subsection, the learning rate and convergence rate of the presented PPO-DRL are discussed. The main objective of DRL algorithms is updating the state-action function $Q(s, a)$ in different ways. The loss function in (18) represents the merits of one chosen control policy. The total loss of PPO and CEM is shown in Fig. 6. The clear downtrends indicate the AEV could achieve better control policy via trial and error procedure. Moreover, the value of loss in PPO is always lower than that in CEM. It means the AEV in the PPO algorithm is more familiar with the driving environment than CEM. Hence, it can be stated that the convergence rate of PPO is better than CEM for the decision-making problem on the highway.

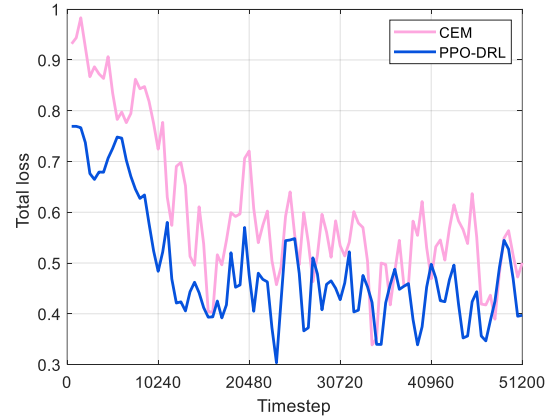


Fig. 6. Value of loss function in two DRL methods: CEM and PPO.

To compare the learning rate of PPO and CEM algorithms, Fig. 7 displays the trajectories of cumulative rewards in these two methods. In (10), the accumulated rewards are the sum of the current reward and discounted future rewards. It is used to estimate the selection of control action. From Fig. 7, the PPO is always bigger than the CEM, which indicates that the control policy derived by PPO is better. The AEV in the PPO method could learn more knowledge and experiences about the driving environment. It is attributed to the new loss function in (18), which enables the intelligent agent to search the optimal control policy faster.

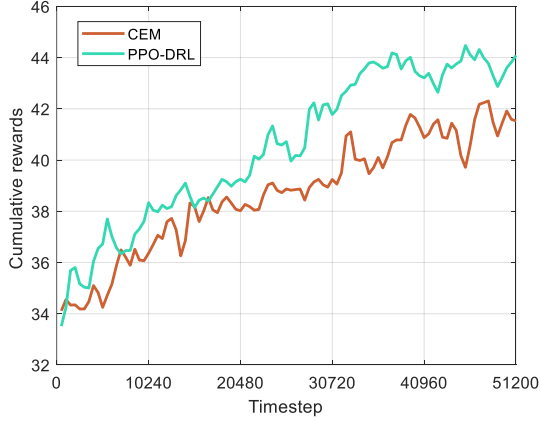


Fig. 7. Accumulated rewards in two compared algorithms: CEM and PPO.

C. Adaptability of PPO DRL

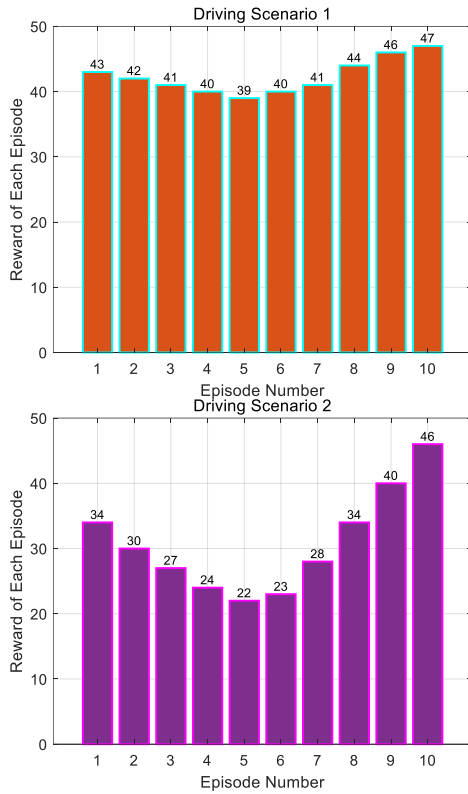


Fig. 8. Rewards in the testing experiments for two new driving scenarios.

This subsection constructs an adaptive estimation framework to verify the proposed decision-making policy. The main factors of one driving scenario are the number of lanes and vehicles. Thus, we change these parameters to establish two new driving scenarios. In the first one, the number of lanes is 4, and the number of vehicles on each lane is 5 (named driving scenario 1). In the second one, the number of lanes is 2, and the vehicle on each lane is 10 (named driving scenario 2). The number of testing episodes for these two new scenarios is 10. The speed and position of these surrounding vehicles are also randomly decided. These driving scenarios represent the uncertainties of the actual driving environments, and they are suitable to clarify the adaptability of the proposed decision-making policy.

Fig. 8 describes the total rewards of PPO in these two new driving scenarios. The higher value of reward means the control policy is more appropriate to this scenario. The lower values of reward are caused by two factors. One is the random position of the surrounding vehicles, which would block all the lanes, and the AEV cannot realize an efficient lane-changing. Another one is that the AEV may implement a dangerous lane-changing in some unusual situations, and will lead to a collision. From Fig. 8, it can be seen that the learned decision-making policy performed better in the first scenario. Because in the first driving scenario, one more lane was added, and the number of surrounding vehicles stayed the same. It indicates the AEV had more choices to achieve lane-changing and avoid a collision. Two individual episodes are chosen and analyzed to expound the adaptability of the proposed decision-making policy.

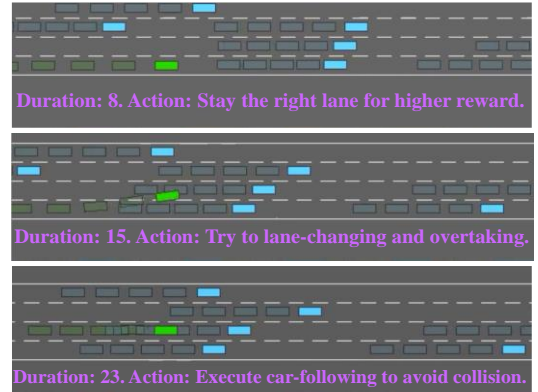


Fig. 9. Episode 5 in driving scenario 1: car-following to avoid collision.

In the new driving scenario 1, episode 5 is selected to analyze due to the lowest value of the reward. As shown in Fig. 9, all the lanes are blocked by the surrounding vehicles for a long time. As a consequence, the AEV has to execute the car-following maneuver to avoid a collision. It implies that the AEV needs to decrease its speed and wait for an opportunity to achieve the overtaking process. Since the reward is affected by the collision condition, vehicle speed, and preferred lane, the value of this episode is a little lower than others. However, this precept is accepted because safety is the most significant concern in the practical driving environment. It also means the learned decision-making policy is able to be adaptive to the mutative driving situation.

Fig. 10 describes the episode 6 in the driving scenario 2 using PPO-DRL-enabled decision-making strategy. It can be noticed that in this scenario, the number of lanes decreases, and the number of vehicles increases. The AEV becomes harder to make decisions as the environments become more complex. From Fig. 10, the AEV made a risky lane-changing when there are many surrounding vehicles. In the training procedure, the AEV may not encounter this situation, so it is hard to predict the future collision. To resolve this problem, two research efforts can be added to enhance the ability of the AEV. One is to prolong the training process to enable the AEV to learn more knowledge from the driving environments. Another is to make the information of surrounding is available to the AEV via communication technology, which helps the AEV to make the right decisions on the highway.

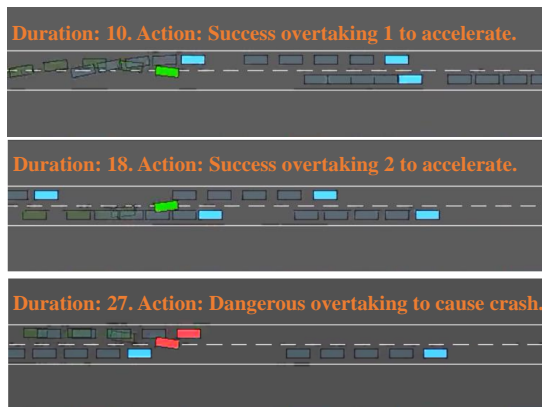


Fig. 10. Episode 6 in driving scenario 2: dangerous overtaking to cause crash.

V. CONCLUSION

In this work, an efficient and safe decision-making policy is presented on the highway for an autonomous vehicle. The special realization method is PPO-DRL. The constructed control framework is generalized to similar driving scenarios with different lanes and surrounding vehicles. Simulation results show that the proposed decision-making could guarantee the optimality, convergence rate, and adaptability. Furthermore, the resulted decision-making is adaptive to different new driving scenarios with disparate performance.

Further works may focus on the online application of the proposed decision-making policy. To add the predicted information for the AEV, it may perform better. Also, the connected environment can be discussed to share the information with nearby vehicles. The real-world collected driving data can be used to evaluate the decision-making in the real-world driving environment.

REFERENCES

- [1] T. Liu, B. Huang, Z. Deng, H. Wang, X. Tang, X. Wang and D. Cao, "Heuristics-oriented overtaking decision making for autonomous vehicles using reinforcement learning", *IET Electrical Systems in Transportation*, 2020.
- [2] A. Rasouli, and J. K. Tsotsos, "Autonomous vehicles that interact with pedestrians: A survey of theory and practice," *IEEE Trans. Intell. Transp. Syst.*, vol. 21, no. 3, pp. 900-918, 2019.
- [3] T. Liu, B. Tian, Y. Ai, L. Chen, F. Liu, and D. Cao, "Dynamic States Prediction in Autonomous Vehicles: Comparison of Three Different Methods," *IEEE Intelligent Transportation Systems Conference (ITSC 2019)*, 27-30 Oct 2019.
- [4] J. Nie, J. Zhang, E. Ding, X. Wan, X. Chen, and B. Ran, "Decentralized cooperative lane-changing decision-making for connected autonomous vehicles," *IEEE Access*, vol. 4, pp. 9413-9420, 2016.
- [5] W. Song, G. Xiong, and H. Chen, "Intention-aware autonomous driving decision-making in an uncontrolled intersection," *Math. Probl. Eng.*, 2016.
- [6] L. Li, K. Ota, and M. Dong, "Humanlike driving: Empirical decision-making system for autonomous vehicles," *IEEE Trans. Veh. Technol.*, vol. 67, no. 8, pp. 6814-6823, 2018.
- [7] C. Hoel, K. Driggs-Campbell, K. Wolff, L. Laine, and M. Kochenderfer, "Combining planning and deep reinforcement learning in tactical decision making for autonomous driving," *IEEE Transactions on Intelligent Vehicles*, vol. 5, no. 2, pp. 294-305, 2019.
- [8] G. Wang, J. Hu, Z. Li, and L. Li, "Cooperative lane changing via deep reinforcement learning," *arXiv preprint arXiv:1906.08662*, 2019.
- [9] Z. Cao, D. Yang, S. Xu, H. Peng, B. Li, S. Feng, and D. Zhao, "Highway Exiting Planner for Automated Vehicles Using Reinforcement Learning," *IEEE Trans. Intell. Transp. Syst.*, 2020.
- [10] N. Sakib. "Highway Lane change under uncertainty with Deep Reinforcement Learning based motion planner," 2020.
- [11] A. Alizadeh, M. Moghadam, Y. Bicer, N. Ure, U. Yavas, and C. Kurtulus, "Automated Lane Change Decision Making using Deep Reinforcement Learning in Dynamic and Uncertain Highway Environment," *In 2019 IEEE Intelligent Transportation Systems Conference (ITSC)*, pp. 1399-1404, 2019.
- [12] S. Zhang, H. Peng, S. Nageshram, and E. Tseng, "Discretionary Lane Change Decision Making using Reinforcement Learning with Model-Based Exploration," *In 2019 18th IEEE International Conference on Machine Learning and Applications (ICMLA)*, pp. 844-850, 2019.
- [13] B. R. Kiran, I. Sobh, V. Talpaert, P. Mannion, A. Sallab, S. Yogamani, and P. Pérez, "Deep reinforcement learning for autonomous driving: A survey," *arXiv preprint arXiv:2002.00444*, 2020.
- [14] J. Kong, M. Pfeiffer, G. Schildbach, and F. Borrelli, "Kinematic and dynamic vehicle models for autonomous driving control design," *In 2015 IEEE Intelligent Vehicles Symposium (IV)*, pp. 1094-1099, June 2015.
- [15] R. Rajamani, *Vehicle Dynamics and Control*, ser. *Mechanical Engineering Series*. Springer, 2011.
- [16] F. Ye, X. Cheng, P. Wang, and C. Chan, "Automated lane change strategy using proximal policy optimization-based deep reinforcement learning," *arXiv preprint arXiv:2002.02667*, 2020.
- [17] M. Treiber, A. Hennecke, and D. Helbing, "Congested traffic states in empirical observations and microscopic simulations," *Phys. Rev. E*, vol. 62, pp. 1805-1824, 2000.
- [18] M. Zhou, X. Qu, and S. Jin, "On the impact of cooperative autonomous vehicles in improving freeway merging: a modified intelligent driver model-based approach," *IEEE Trans. Intell. Transp. Syst.*, vol. 18, no. 6, pp. 1422-1428, June 2017.
- [19] A. Kesting, M. Treiber, and D. Helbing, "General lane-changing model MOBIL for car-following models," *Transportation Research Record*, vol. 1999, no. 1, pp. 86-94, 2007.
- [20] T. Liu, X. Hu, W. Hu, Y. Zou, "A heuristic planning reinforcement learning-based energy management for power-split plug-in hybrid electric vehicles," *IEEE Trans. Ind. Inform.*, vol. 15, no. 12, pp. 6436-6445, 2019.
- [21] T. Liu, X. Tang, H. Wang, H. Yu, and X. Hu, "Adaptive Hierarchical Energy Management Design for a Plug-in Hybrid Electric Vehicle," *IEEE Trans. Veh. Technol.*, vol. 68, no. 12, pp. 11513-11522, 2019.
- [22] T. Liu, B. Wang, and C. Yang, "Online Markov Chain-based energy management for a hybrid tracked vehicle with speedy Q-learning," *Energy*, vol. 160, pp. 544-555, 2018.
- [23] T. Liu, H. Yu, H. Guo, Y. Qin, and Y. Zou, "Online energy management for multimode plug-in hybrid electric vehicles," *IEEE Trans. Ind. Inform.*, vol. 15, no. 7, pp. 4352-4361, July 2019.
- [24] J. Duan, S. E. Li, Y. Guan, Q. Sun, and B. Cheng, "Hierarchical reinforcement learning for self-driving decision-making without reliance on labelled driving data," *IET Intell. Transp. Syst.*, vol. 14, no. 5, pp. 297-305, 2020.
- [25] M. L. Puterman, "Markov decision processes: discrete stochastic dynamic programming," *John Wiley & Sons*, 2014.
- [26] X. Hu, T. Liu, X. Qi, and M. Barth, "Reinforcement learning for hybrid and plug-in hybrid electric vehicle energy management: Recent advances and prospects," *IEEE Ind. Electron. Mag.*, vol. 13, no. 3, pp. 16-25, 2019.
- [27] J. Schulman, F. Wolski, P. Dhariwal, A. Radford, and O. Klimov, "Proximal policy optimization algorithms," *arXiv preprint arXiv:1707.06347*, 2017.
- [28] J. Schulman, S. Levine, P. Abbeel, M. Jordan, and P. Moritz, "Trust region policy optimization," *In International conference on machine learning*, pp. 1889-1897, 2015.
- [29] L. Edouard, "An environment for autonomous driving decision-making," <https://github.com/eleurent/highway-env>, *GitHub*, 2018.
- [30] I. Szita and A. L'orincz, "Learning Tetris using the noisy cross-entropy method," *In: Neural computation*, vol. 18, no. 12, pp. 2936-2941, 2006.



Xin Ye received the B.S. degree in Mechanical Engineering from Chongqing University, China in 2004; and the Ph.D degree in Vehicle Engineering from Chongqing University, China in 2011. She is currently an associate professor with the School of Vehicle Engineering, Chongqing University of Technology, Chongqing 400054, China.

Her research fields include new energy and intelligent vehicle integrated control, intelligent algorithm research and so on.



Xiaolin Tang received a B.S. in mechanics engineering and an M.S. in vehicle engineering from Chongqing University, China, in 2006 and 2009, respectively. He received a Ph.D. in mechanical engineering from Shanghai Jiao Tong University, China, in 2015. From August 2017 to August 2018, he was a visiting professor of Department of Mechanical and Mechatronics Engineering, University of Waterloo, Waterloo, ON, Canada. He is currently an Associate Professor at the College of Mechanical and

Vehicle Engineering, Chongqing University, Chongqing, China. He is also a committeeman of Technical Committee on Vehicle Control and Intelligence of Chinese Association of Automation (CAA). He has led and has been involved in more than 10 research projects, such as National Natural Science Foundation of China, and has published more than 30 papers. His research focuses on Hybrid Electric Vehicles (HEVs), vehicle dynamics, noise and vibration, and transmission control.



Kang Yu received the B.E. degree in Vehicle Engineering from Chongqing University of Technology, China in 2021. He is currently pursuing the MA.Eng. degree in Vehicle Engineering with Chongqing University of Technology, Chongqing 400054, China.

His research fields include new energy and intelligent vehicle integrated control, intelligent algorithm research and so on.